Control Algorithms to Mitigate the Effect of Uncertainties in Residential Demand Management

Gayan Lankeshwara[a], Rahul Sharma [a,*], Ruifeng Yan[a], Tapan K. Saha[a]

[a]*School of Information Technology and Electrical Engineering, The University of Queensland, Brisbane, QLD 4072, Australia.*

Abstract

Uncertainties at end-user and aggregator levels can be highly detrimental to the practical implementation of residential load control schemes for electricity market applications. Uncertainty factors such as end-user non-compliance, comfort violations and load set-point changes associated with the demand response aggregator are unavoidable in practice. This paper proposes a novel two-stage control algorithm for robust centralised management of aggregate residential loads which guarantee precise load set-point tracking in the presence of uncertainties occurring in real-time while ensuring that end-user thermal comfort is not compromised. The approach is underpinned by optimal selection of appliances based on an emulated supply curve followed by solving a one-step-ahead optimisation problem. Using air conditioners and water heaters as the controllable loads, the paper illustrates the effectiveness of the proposed approach in load management whilst mitigating the effects of unknown uncertainties. Further, the developed control scheme is compared with an existing industry approach. The results yield that the proposed control scheme is robust to uncertainties, preserves thermal comfort and is applicable for practical implementation under existing demand response standards.

Keywords: Uncertainty, direct load control, customer non-compliance, demand response aggregator, grid services, optimisation

*Corresponding author

Email addresses: g.lankeshwara@uqconnect.edu.au (Gayan Lankeshwara), rahul.sharma@uq.edu.au (Rahul Sharma), ruifeng@itee.uq.edu.au (Ruifeng Yan), saha@itee.uq.edu.au (Tapan K. Saha)

Nomenclature

$\mathcal{A}$	set of appliance indexed by i
Ω_{AC}	set of air conditioners
Ω_{EWH}	set of water heaters
$\overline{T}_i^{\text{outlet}}$	upper set point for the EWH in house i (°F)
$\overline{T}_i^{\text{room}}$	upper set point for the AC in house i (°F)
$\underline{T}_i^{\text{outlet}}$	lower set point for the EWH in house i (°F)
$\underline{T}_i^{\text{room}}$	lower set point for AC the in house i (°F)
ζ	set of priority clusters indexed by χ_j
n_a	number of appliances in each house
N_h	number of houses
P_{req}	Required demand response
$P_{i,t}^{\text{AC}}$	power input to the air conditioner i at time t
$P_{i,t}^{\text{EWH}}$	power input of the water heater i at time t
T_{dur}	Duration of demand response event
$T_{i,t}^{\text{outlet}}$	outlet temperature of water heater i at time t (°F)
$T_{i,t}^{\text{room}}$	room temperature for the air conditioner i at time t (°F)
t_s	duration of time slot

1. Introduction

With the rapid proliferation of highly intermittent renewable energy sources such as solar, wind in the generation mix, the grid operators are currently faced with immense challenges in maintaining the stability and safe operation of the grid while mitigating supply-demand imbalances in real-time [1]. Although conventional approaches such as network capacity upgrades and reinforcements, spinning reserves have succeeded in addressing these challenges, their high capital costs and high investment periods have paved the path for grid operators to explore non-conventional measures of reserve provision. To this end, demand management schemes have gained much popularity within the power research community due to recent developments in two-way communication and advanced metering infrastructure (AMI) at the consumer end [2].

Direct Load Control (DLC) [3, 4] is one such promising demand management technique adopted by utilities or third-parties. In this approach, the end-customers allow the utilities to control the consumption of household appliances and receive incentives as compensation for their contribution in demand management events.

To date, a substantial amount of published work is available on the DLC capabilities of thermostatically controllable appliances. For example, the authors in [5] have proposed a collective control approach for residential Heating-Ventilation-Air-Conditioning (HVAC) based on a combination of greedy algorithm and a binary search algorithm while preserving customer-chosen temperature limits. A centralised control scheme is proposed in [6] for an aggregate heterogeneous population of air conditioners where the control action addresses compressor "lock-out" effect. The authors in [7] have proposed a state bin transition model and developed a probabilistic control scheme for air conditioners to provide regulation services. A sliding mode control scheme is introduced in [8] for the real-time control of air conditioning loads through a universal temperature set-point strategy. An HVAC control scheme coordinated with battery storage is presented in [9] to obtain flexibility for demand management while ensuring thermal comfort for end-users. The authors in [10] have introduced an efficient and scalable aggregate control framework where the solution to a multi-objective optimisation problem determines control set-points for air conditioners and water heaters. In [11], the authors have attempted to quantify the flexibility of an electric water heater aggregator and proposed a control scheme based on the mean-field approach. Despite the success of most of the proposed approaches in delivering desired capacity without compromising customer comfort, still these control schemes require guaranteed participation of end-users during a demand management event. Con-

sequently, most of the approaches fail to deliver desired outcomes in the event of end-user non-compliance.

On the other hand, a plethora of literature is available on demand management in the presence of uncertainties. However, most of the studies have only focussed on uncertainties due to thermal model mismatches [12, 13] and uncertainties due to forecast errors [14, 15]. For instance, the authors in [12] have developed a robust model predictive control (MPC) scheme to optimise the energy consumption of a building while accounting for uncertainties in parameters of the building thermal model. In [14], the authors have proposed an offline stochastic optimisation approach for demand management under uncertain outdoor temperature forecasts whereas a stochastic MPC approach is proposed in [15] for building climate control in real-time under uncertain outdoor temperature. Nonetheless, most of these approaches have not been able to establish the end-user behaviour in accomplishing desired demand management in an event. Despite the attempt to model the uncertainty in end-user behaviour in [16, 17], the approach is only valid for modelling the uncertainty in non-controllable load consumption and inapplicable for modelling end-user non-compliance in real-time. A summary of the existing literature on demand management in the presence of uncertainties is given in Table 1.

Thus far, only a handful of studies have dealt with achieving desired demand reduction in the presence of customer non-compliance action. Although the authors in [39, 40] have highlighted the importance of addressing non-compliance in the formulation, no explicit modelling has been attained while developing control algorithms. Even though a high-level modelling of non-compliance based on Markov-chains is proposed in [38], the authors have focussed only on non-compliance at household level but not at individual appliance level. Nevertheless, the studies conducted in [41, 42] have pointed out that enabling an override option or external control action induces end-user's "perceived control" even though a utility or an aggregator actually controls the consumption of household appliances. Hence, to be competitive with real-world implementation, it is vital to develop load control schemes which not only ensure customer comfort but also account for end-user voluntary compliance.

Meantime, enabling end-user voluntary compliance creates complexities when an aggregator provides services in electricity markets. As per the existing market policies, the commitment is mandatory for an aggregator if its bids are cleared [43]. However, in the event of a significant override, there is no guarantee that the aggregator will be able to deliver desired bids, which ultimately leads to penalties for non-compliance. The demand response (DR) trial conducted by the Australian

Table 1. Comparison of existing approaches for demand management in the presence of uncertainties

Ref.	**Application**	**Uncertainty**				
		Occupancy [a]	Non-compliance [b]	Temp. violations [c]	Set-point changes	Weather forecasts
[14]	DAS	×	×	×	–	✓
[15]	RTC	×	×	×	–	✓
[16]	DAS	✓	×	×	–	✓
[17]	DAS	✓	×	×	–	✓
[18]	DAS	×	×	×	–	✓
[19]	DAS	✓	×	×	–	✓
[20]	DAS	×	×	–	–	✓
[21]	DAS	×	✓	–	–	–
[22]	DAS	×	✓	–	–	✓
[23]	DAS	✓	×	×	–	✓
[24]	DAS	✓	✓	–	–	✓
[25]	DAS	×	×	×	–	✓
[26]	DAS and RTC	✓	×	–	–	✓
[27]	DAS and RTC	✓	×	–	–	✓
[28]	DAS and RTC	✓	✓	–	–	✓
[29]	RTC	✓	×	–	–	✓
[30]	RTC	✓	×	–	–	✓
[31]	RTC	✓	×	×	–	✓
[32]	RTC	×	–	–	–	✓
[33]	RTC	✓	×	–	–	×
[34]	RTC	✓	×	–	–	–
[35]	RTC	×	×	×	×	✓
[36]	RTC	×	×	–	–	–
[37]	RTC	✓	×	–	–	✓
[38]	RTC	✓	✓	–	–	–
proposed	*RTC*	✓	✓	✓	✓	–

'✓' : considered, '×' : not considered, '–' not-applicable
DAS – day-ahead scheduling; RTC – real-time control
[a] occupancy is related to non-controllable loads
[b] non-compliance is related to controllable loads
[c] temperature violations due to end-user discomfort (related to non-compliance of HVAC)

Energy Market Operator (AEMO) in 2019 [44], gives evidence of such a non-compliance event at the level of residential customers during an emergency DR event. To add more, DLC programs conducted across the world [45] have recorded

significant customer non-compliance events during the operation. Hence, there is no doubt that a systematic approach is essential if residential aggregators are to participate in markets and maximise social welfare in the presence of real-time uncertainties.

Fig. 1 represents a simulated scenario to illustrate the effect of customer override on the overall performance of a DR event. The simulation is based on the data obtained from [46] and shows the divergence of actual consumption from its expected value due to the override of DR commands by customers.

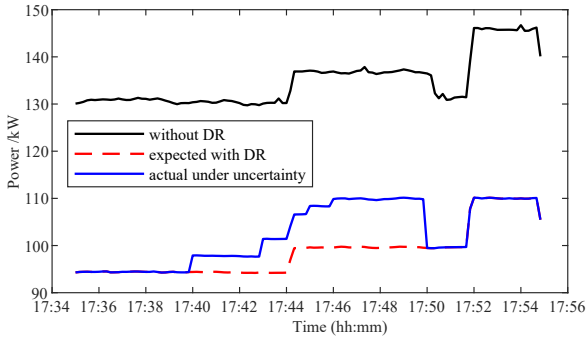

Fig. 1. A simulated scenario showing the overall effect of end-user non-compliance on the performance of a DR event

On the other hand, the existing DLC approaches usually rely on broadcast control where identical control set-point signals are sent to all participating units regardless of their state of operation or the level of comfort [47]. This leads to uneven variations of comfort which could end up some appliances being operated out of their comfort zones. Thereby, most of the end-users tend to override the control action with the intention of regaining their comfort.

Moreover, the previous studies have predominantly focussed on control schemes for regular ON-OFF type air conditioners [5, 7]. However, with the growing demand for inverter-type air conditioners [48], the applicability of previous work based on regular ON-OFF type air conditioners remains a question. To add more, the current demand response standards, e.g., AS/NZS 4755 standards in Australia [49], is only applicable for inverter-type air conditioners [50]. Hence, there is always a need for control schemes compatible with modern smart home appliances and at the same time consistent with existing demand response standards.

Knowledge gap

The knowledge gap is summarised as follows:

- The effect of uncertainties is generally ignored while developing residential load control schemes for electricity market applications. However, demand management methods that do not explicitly consider uncertainties are unlikely to perform as expected in practical settings.
- The inverter-type air conditioners operating under demand response standards have received little attention compared to regular ON-OFF type air conditioners in the state-of-the-art load control algorithms.
- The existing load control programs have only focussed on broadcast control where all the participating units receive an identical control signal from a central entity at a certain time.

Main contributions

Motivated by the gaps in the existing literature and the outcomes of industrial DR trials, it is understood that a DR scheme resembling near real-time implementation while accounting for possible scenarios of uncertainty is highly deemed to achieve precise load control while managing the comfort for the end customers. Aligned with this, the main contributions of this work are:

- *Development of control schemes to account for uncertainties*: Control algorithms are developed for a demand response aggregator to achieve precise load set-point tracking while accounting for uncertainties at end-user and aggregator levels in real-time operation arising from:
  - Customer non-compliance events
  - End-user temperature comfort violations during an event
  - System operator's decision to change the load-set point reduction
- *Compatibility with existing demand response standards*: The developed control scheme ensures continuous end-user thermal comfort during the event and applicable with modern residential thermostatically controllable loads (TCLs) under existing demand response standards.
- *Emulation of supply-curve in electricity markets for optimal selection of appliances*: Unlike broadcast control in the majority of the existing demand response programs, the proposed control scheme utilises a novel two-stage control approach for optimal appliance selection which involves a priority-evolved stacking of appliances emulating a supply-curve in electricity markets and solving a one-step-ahead optimisation problem. To this end, the

proposed two-stage control scheme is computationally tractable even under explicit consideration of discrete power consumption levels (demand response standards) for TCLs.

- *Tracking performance under existing demand response standards:* The proposed control scheme is able to achieve the same level of tracking performance of a non-explicit controller even the consumption of TCLs are restricted to explicit discrete levels under existing demand response standards.

The rest of the paper is organised as follows. Section 2 provides a detailed description of the overall system model and formulates the problem for the DR aggregator. Section 3 describes the proposed methodology, priority-evolved stacking of appliances and supply curve based decision-making in section 3.1, one-step-ahead optimisation problem in section 3.2 and the overall control scheme to address uncertainties in section 3.4. Section 4 presents simulation results to validate the proposed approach and section 5 concludes the paper.

2. System Model & Problem Formulation

It is assumed that the aggregator is responsible for N_h houses in a particular geographical area and each house is equipped with an inverter type air conditioner (AC) and an electric storage water heater (EWH). Fig. 2 summarises the overall control architecture of the proposed approach.

According to Fig. 2, the aggregator receives control signals $\{P_{\text{req}}, T_{\text{dur}}\}$ from the system operator according to its participation in either wholesale markets or contracts. Here, P_{req} is the contracted power reduction by the aggregator during a certain DR event and T_{dur} is the duration of that particular event. Depending on the application of DR such as peak shaving or regulation of service, T_{dur} could vary from several minutes to hours. Nonetheless, the main contribution of this work is devising a controller for the aggregator to provide desired demand reduction during an event. After receiving the information regarding the DR event, the DR controller executes its own algorithm to control appliances sequentially in multiple steps. The step size of each time slot is represented as t_s.

As shown in Fig. 2, the DR controller generates set-points for each cluster at each time instant during a demand reduction event. Following this, a modelling framework comprising key aspects of smart energy hubs (SEHs) [51–53] is utilised to achieve combined demand reduction from ACs and EWHs.

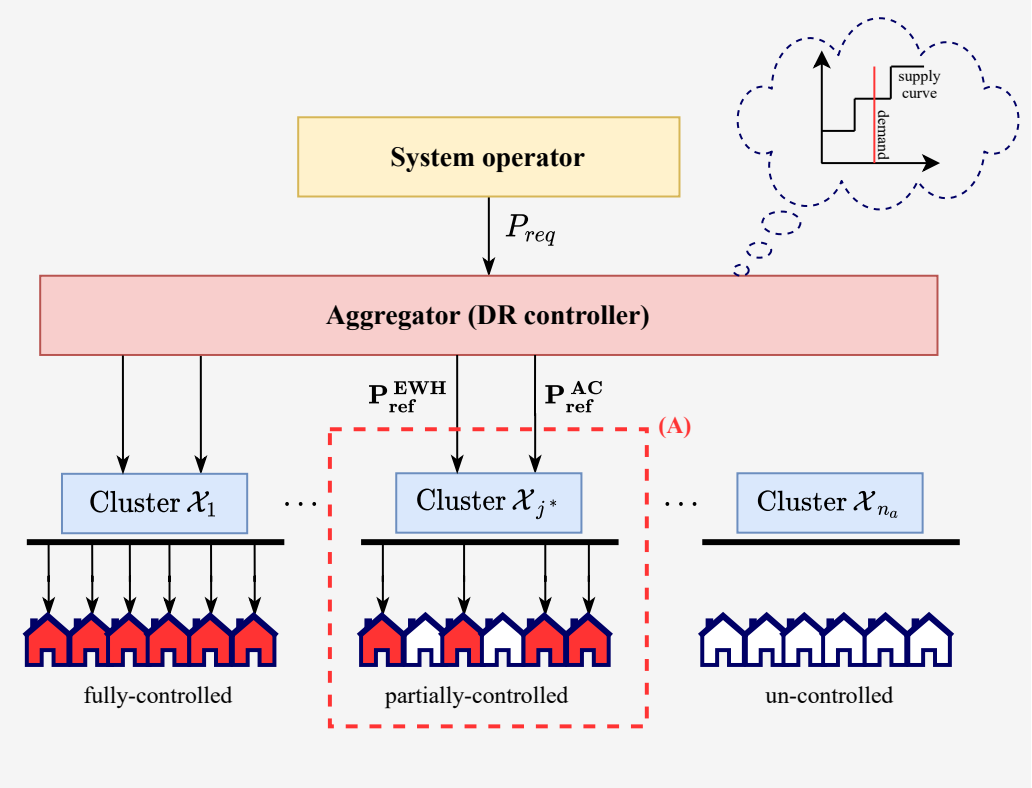

Fig. 2. A high-level diagram representing the overall control architecture: the novel supply-curve based decision-making process for the DR controller results in priority cluster-based control where devices are fully controlled in lower-priority clusters, partially controlled in the marginal cluster whereas uncontrolled in remaining clusters; the highlighted portion (A) is further described in Fig. 3

Fig. 3 represents the sub-system based control implementation in a certain cluster following the SEH framework. According to Fig. 3, the DR controller generates separate reference power consumption set-points for the air conditioning and water heating subsystems in a particular cluster. The input $\mathbf{P}_{\text{ref}}^{\text{AC}} = \{P_{\text{ref},i,t}^{\text{AC}} \,|\, \forall\, i \in \Omega_{\text{AC}}\}$ to the air conditioning subsystem corresponds to the controller assigned reference power levels for ACs at time t. Similarly, $\mathbf{P}_{\text{ref}}^{\text{EWH}} = \{P_{\text{ref},i,t}^{\text{EWH}} \,|\, \forall\, i \in \Omega_{\text{EWH}}\}$ corresponds to the reference power levels for EWHs at time t. The outputs of the cluster are $\mathbf{P}_{\text{out}}^{\text{AC}}$: output electrical power consumption of ACs in the subsystem, $\mathbf{P}_{\text{out}}^{\text{EWH}}$: output electrical power consumption of EWHs in the subsystem.

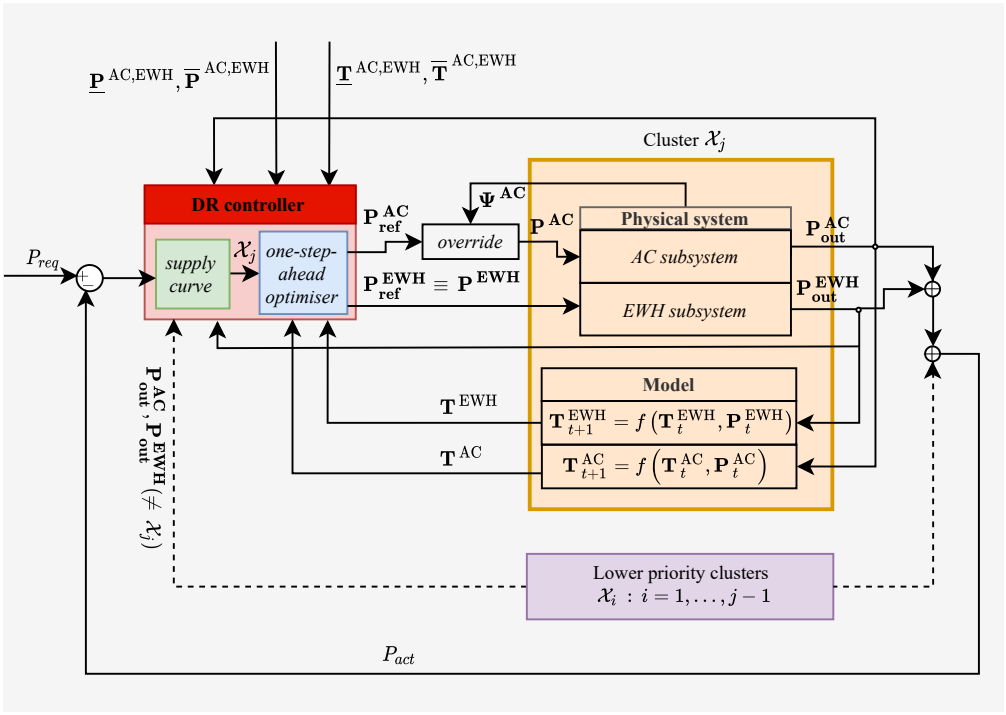

Fig. 3. A detailed block diagram showing the control implementation in cluster $\mathcal{X}_j$ for air-conditioning and water heating subsystems based on smart energy hubs framework; control actions in lower priority clusters are not shown.

2.1. Air conditioning subsystem

As shown in Fig. 3, the input to the air conditioning subsystem $\mathbf{P}^{\mathrm{AC}}_{\mathbf{ref}}$ passes through the AC override block to give the output $\mathbf{P}^{\mathrm{AC}} = \{P^{\mathrm{AC}}_{i,t} \,|\, \forall\, i \in \Omega_{\mathrm{AC}}\}$ which is the power consumption of ACs at time t. The power consumption of the i^{th} AC at time t, $P^{\mathrm{AC}}_{i,t}$, is measured in kW and bounded such that $\{\underline{P}^{\mathrm{AC}}_{i} \leq P^{\mathrm{AC}}_{i,t} \leq \overline{P}^{\mathrm{AC}}_{i}\,; \forall\, i \in \Omega_{\mathrm{AC}}\}$.

The AC override vector $\mathbf{\Psi}^{\mathrm{AC}} = \{\psi^{\mathrm{AC}}_{i,t} \,|\, \forall\, i \in \Omega_{\mathrm{AC}}\}$ contains the override state of ACs at time t. The override state of the i^{th} AC at time t which is $\psi^{\mathrm{AC}}_{i,t}$ can only be 0 or 1. $\psi^{\mathrm{AC}}_{i,t} = 1$ denotes that AC i has overridden the control signal sent at time t and opted-out from the DR event, whereas $\psi^{\mathrm{AC}}_{i,t} = 0$ corresponds to the absence of an overriding event and the AC operates at the reference consumption

level assigned by the controller at time t. This can be expressed as,

$$\psi_{i,t}^{\mathrm{AC}} = \begin{cases} 0 & \text{if} \quad P_{i,t}^{\mathrm{AC}} = P_{\mathrm{ref},i,t}^{\mathrm{AC}} \\ 1 & \text{if} \quad P_{i,t}^{\mathrm{AC}} \neq P_{\mathrm{ref},i,t}^{\mathrm{AC}} \end{cases} \tag{1}$$

The state vector $\mathbf{T}^{\mathrm{AC}} = \{T_{i,t}^{\mathrm{room}} \,|\, \forall\, i \in \Omega_{\mathrm{AC}}\}$ consists of room temperature of ACs at time t. Moreover, $T_{i,t}^{\mathrm{room}}$ is measured in °F and bounded s.t. $\{\underline{T}_i^{\mathrm{room}} \leq T_{i,t}^{\mathrm{room}} \leq \overline{T}_i^{\mathrm{room}}\ ; \forall\, i \in \Omega_{\mathrm{AC}}\}$ where $\underline{T}_i^{\mathrm{room}}$ and $\overline{T}_i^{\mathrm{room}}$ are the minimum and maximum permissible room temperature for the i^{th} AC. The output is $\mathbf{P}_{\mathrm{out}}^{\mathrm{AC}} = \{P_{\mathrm{out},i,t}^{\mathrm{AC}} \,|\, \forall\, i \in \Omega_{\mathrm{AC}}\}$ which is the output power consumption of ACs at time t.

2.1.1. Indoor temperature modelling for inverter air conditioners

Fig. 4 represents a detailed model of an inverter-type air conditioner [54] where T^{outdoor} is the outdoor temperature; T^{set} is the set-point temperature; T^{room} is the indoor temperature; P^{AC} is the electric power; Q^{AC} is the cooling power; P_d is the unconstrained electric power; P_{sat}^{+} and P_{sat}^{-} are the upper saturation limit and lower saturation limit respectively. In addition to that, the DRM input represents the demand response modes under which an air conditioner can operate during a DR event.

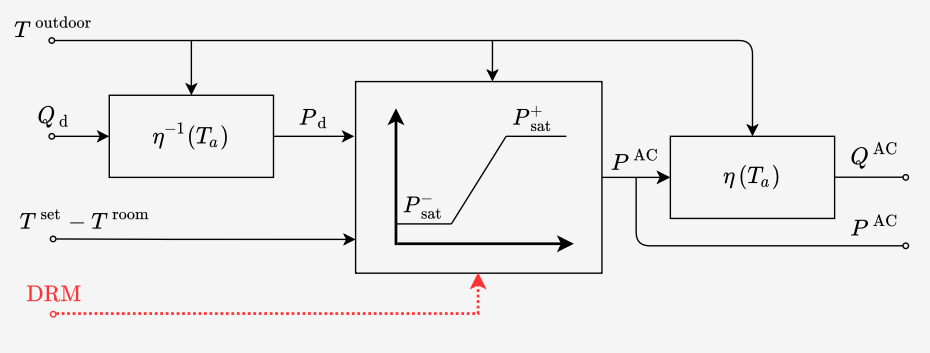

Fig. 4. A detailed model of an inverter-type air conditioner [54]

Unlike a two-stage on-off compressor type air conditioner, an inverter air conditioner can operate under different power consumption levels by adjusting its compressor frequency to reach the desired set-point. This can be mathematically expressed as [48]:

$$Q_{i,t}^{\mathrm{AC}} = \kappa_Q \cdot f_{i,t} + \mu_Q \tag{2}$$

$$P_{i,t}^{\mathrm{AC}} = \kappa_P \cdot f_{i,t} + \mu_P \tag{3}$$

where $Q_{i,t}^{\mathrm{AC}}$ is the cooling power in kW, $P_{i,t}^{\mathrm{AC}}$ is the electrical power input in kW and $f_{i,t}$ is the compressor frequency in Hz of the i^{th} air conditioner at time t. Considering residential environments where the required cooling capacity varies from 2 $\sim$ 7 kW, the compressor frequency varies between 20 $\sim$ 150 Hz [48]. Furthermore, κ_Q, μ_Q, κ_P, μ_P represent the constant coefficients for inverter air conditioners. For inverter air conditioners with cooling capacity in the range 0.5 $\sim$ 5 kW, κ_Q = 0.06 kW/Hz, μ_Q = -0.3 kW, κ_P = 0.03 kW/Hz and μ_P = -0.4 kW [48].

Aligned with the operation of an inverter-type air conditioner during a DR event, a simplified thermal model [55] which represents an intermediate stage of the overall control operation given in Fig. 4 is utilised in this work. Considering the cooling mode for air conditioner $i \in \Omega_{\mathrm{AC}}$ at time t, this can be expressed as,

$$T_{i,t+1}^{\mathrm{room}} = T_{i,t}^{\mathrm{room}} + t_s \cdot \frac{G_{i,t}}{\Delta c_i} - t_s \cdot \frac{Q_{i,t}^{\mathrm{AC}}}{\Delta c_i} \tag{4}$$

where $G_{i,t}$ is the heat gain rate of house at time t measured in Btu/h and Δc_i is the energy required to change the temperature of the air inside the room by 1°F measured in Btu/°F. Furthermore, $G_{i,t}$ can be obtained by,

$$G_{i,t} = \left(\frac{A_i^{\mathrm{wall}}}{R_i^{\mathrm{wall}}} + \frac{A_i^{\mathrm{ceil}}}{R_i^{\mathrm{ceil}}} + \frac{A_i^{\mathrm{win}}}{R_i^{\mathrm{win}}} + 11.77 \cdot \eta_{\mathrm{ac}} \cdot V_i^h\right) \times (T_{i,t}^{\mathrm{outdoor}} - T_{i,t}^{\mathrm{room}}) + \mathrm{SHGC} \cdot A_i^{\mathrm{sw}} \cdot H^s \cdot \frac{3.412}{10.76} + H_i^p \tag{5}$$

where A^{wall}, A^{ceil}, A^{win} and A^{sw} are the area of the walls, ceilings, windows and south-windows in ft^2 respectively. R^{wall}, R^{ceil}, R^{win} are the thermal resistance of walls, ceilings and windows in °F $\cdot$ ft^2 $\cdot$ h /Btu. η_{ac} is the number of air changes per hour (1/h), V^h is the volume of the house in ft^3. T^{outdoor} is the outdoor air temperature in °F, SHGC is the solar heat gain coefficient of windows, H^s is the solar radiation of heat power in W/m^2 and H^p is the heat gain from people in Btu/h. In addition to that Δc_i can be expressed as,

$$\Delta c_i = C^{\mathrm{air}} \cdot V_i^h \tag{6}$$

where C^{air} is the specific heat capacity of air in Btu/ft^3 $\cdot$ °F. The typical values of thermal parameters in (4), (5) and (6) are obtained from [55] and [56]. A summary of thermal parameters in (4) and (5) is given in Appendix A.

2.2. Water heating subsystem

Unlike for the air conditioning subsystem, no overriding capabilities are enabled for EWHs in practice. With this assumption, as shown in Fig. 3, the central controller defined set-points for EWHs $\mathbf{P}_{\text{ref}}^{\text{EWH}}$ directly pass through as inputs to the water heating subsystem which is given by $\mathbf{P}^{\text{EWH}} = \{P_{i,t}^{\text{EWH}} \,|\, \forall\, i \in \Omega_{\text{EWH}}\}$. Furthermore, the power consumption of the i^{th} EWH at time t, $P_{i,t}^{\text{EWH}}$, is measured in kW and bounded such that $\{\underline{P}_i^{\text{EWH}} \leq P_{i,t}^{\text{EWH}} \leq \overline{P}_i^{\text{EWH}}; \forall\, i \in \Omega_{\text{EWH}}\}$ where $\underline{P}_i^{\text{EWH}}$ and $\overline{P}_i^{\text{EWH}}$ are the minimum and maximum permissible power consumption.

The state vector $\mathbf{T}^{\text{EWH}} = \{T_{i,t}^{\text{outlet}} \,|\, \forall\, i \in \Omega_{\text{EWH}}\}$ consists of temperature of EWHs at time t where $T_{i,t}^{\text{outlet}}$ is measured in °F and bounded such that $\{\underline{T}_i^{\text{outlet}} \leq T_{i,t}^{\text{outlet}} \leq \overline{T}_i^{\text{outlet}}; \forall\, i \in \Omega_{\text{EWH}}\}$ and $\underline{T}_i^{\text{outlet}}$ and $\overline{T}_i^{\text{outlet}}$ are the minimum and maximum permissible outlet water temperature for the i^{th} water heater. The output vector is $\mathbf{P}_{\text{out}}^{\text{EWH}} = \{P_{\text{out},i,t}^{\text{EWH}} \,|\, \forall\, i \in \Omega_{\text{EWH}}\}$ which is the output power consumption of EWHs at time t.

2.2.1. Temperature modelling for electric water heaters

This work considers electric storage type water heaters. The standards introduced in [49] admit that EWHs can operate under discrete power consumption levels during a DR event. Hence, the thermal model in [55] is reshaped for the i^{th} water heater at time t as,

$$T_{i,t+1}^{\text{outlet}} = T_{i,t}^{\text{outlet}} \cdot \frac{(V_i^{\text{tank}} - f_{i,t}^{r} \cdot t_s)}{V_i^{\text{tank}}} + \frac{T_i^{\text{inlet}} \cdot f_{i,t}^{r} \cdot t_s}{V_i^{\text{tank}}} + \frac{1}{8.34} \cdot \left(P_{i,t}^{\text{EWH}} \times 3412 \; - \frac{A_i^{\text{tank}} \cdot (T_{i,t}^{\text{outlet}} - T_{i,t}^{\text{amb}})}{R_i^{\text{tank}}} \right) \cdot \frac{t_s}{60} \cdot \frac{1}{V_i^{\text{tank}}} \quad (7)$$

where V^{tank} is the volume of the tank in gallons, A^{tank} is the area of the tank in ft^2, R^{tank} is the thermal resistance of the tank in °F $\cdot$ ft^2 $\cdot$ h /Btu. Furthermore, $f_{i,t}^{r}$ is the flow-rate in gal/min at time t, $T_{i,t}^{\text{inlet}}$ is the inlet temperature of the water heater in °F at time t and $T_{i,t}^{\text{amb}}$ is the ambient room temperature in °F at time t. Similar to the thermal model for the air conditioner, the parameters described in (7) are extracted from [55] and [57]. A summary of thermal parameters in (7) is given in Appendix A.

2.3. Problem formulation

Consider a scenario where the system operator foresees a supply-demand mismatch and informs the aggregator to provide P_{req} of DR within T_{dur} of time. The

choice of the specific aggregator could be from bidding in wholesale markets or bi-lateral contracts. The objective of this work is for the aggregator to achieve P_{req} in the presence of uncertainties discussed in section 1 while maintaining the level of comfort for customers. In achieving the overall objective, the optimal selection of appliances, algorithm development in the presence of uncertainties are discussed in section 3.

3. Proposed Methodology

Let us consider an aggregator responsible for controlling the consumption of appliances in N_h households to successfully achieve P_{req} within T_{dur} of time. In doing so, it is assumed that the DR controller has knowledge on the near real-time consumption of customer-owned controllable appliances. Meantime, customers provide information to the aggregator on the desired limits of operation for appliances, e.g., lower and upper thermal set-points for ACs [$\underline{T}^{\text{room}}, \overline{T}^{\text{room}}$], lower and upper thermal set-points for EWHs [$\underline{T}^{\text{outlet}}, \overline{T}^{\text{outlet}}$]. Furthermore, it is assumed that the DR controller has information on thermal models of each household. Although the direct approach where the aggregator collects information from each house is trivial and inconsistent, a growing body of literature on indirect approaches such as grey-box and black-box parameter estimation [58, 59] and learning-based approaches [13, 60] provide solid evidence that these aforementioned indirect methods are applicable in real-world implementation. A summary of variables used to formulate the overall problem is given in Table 2.

Table 2. A description of variables used to formulate the problem

Variable	Description
$P_{\text{req,t}}$	required demand reduction at time t
$P_{i,t}^{AC}$	power consumption of i^{th} air conditioner at time t
$P_{i,t}^{EWH}$	power consumption of i^{th} water heater at time t
$\Delta P_{i,t}^{AC}$	power reduction of i^{th} air conditioner at time t
$\Delta P_{i,t}^{EWH}$	power reduction of i^{th} water heater at time t
$T_{i,t}^{\text{room}}$	room temperature for i^{th} air conditioner at time t
$T_{i,t}^{\text{outlet}}$	outlet temperature for i^{th} water heater at time t

In order to provide more flexibility to end-customers, an emulation of a supply curve in electricity markets with cascading priority clusters is accompanied in the dispatch process.

3.1. Conceptual priority-based ranking mechanism and emulated supply curve formation

Consider n_a number of controllable appliances present in each house $h \in \{1, \ldots, N_h\}$. For each appliance $i \in \mathcal{A}$, a customer is required to define a priority index j s.t. $j \in \{1, \ldots, n_a\}$. The priority index j is used as a quantitative measure of the importance of an appliance over the others. For example, if the customer in house h assigns priority index $j = 1$ to the EWH and priority index $j = 2$ to the AC, it implies that the operation of the AC is more critical than the EWH during a DLC event.

Once j is assigned for $\forall\, i \in \mathcal{A}$ by the customers in $\forall\, h \in \{1, \ldots, N_h\}$, a set of priority orders ζ is defined s.t. $\zeta = \left\{\mathcal{X}_j \,|\, j \in \{1, \ldots, n_a\}\right\}$ where $\mathcal{X}_j$ corresponds to priority cluster formed by the appliances with priority index j. In practice, most of the existing DLC approaches do not allow an appliance to be fully controlled (turned off), instead allow a minimum consumption level which is usually a fraction of the rated power [49]. Thus, the flexible power of an appliance, which is the maximum demand reduction that can be achieved from an appliance will differ from its rated capacity. Adhering to this, the flexible power of an appliance i at a time t can be expressed as, $P^{\text{flex}}_{i,t} = (1 - K) \times P_{i,\text{rated}}$ where K is the minimum fraction of power that should be allocated for an appliance. Based on the flexibility of appliances, the total flexible power of cluster $\mathcal{X}_j$ at time t can be expressed as,

$$P^{\text{flex}}_{\mathcal{X}_j,t} = \sum_i P^{\text{flex}}_{i,t} \qquad \forall i \in X_j \tag{8}$$

Likewise, for $\forall \mathcal{X}_j$, the aggregated flexible power at time t can be cascaded in an increasing priority order to form an emulated supply curve shown in Fig. 5.

Inspired by the determination of the clearing price based on the intersection between the supply curve and the demand curve in electricity markets, a similar approach is followed to determine the marginal cluster $\mathcal{X}_{j^*}$ and non-marginal lower priority clusters $\mathcal{X}_j$ for $j \in \{1, 2 \ldots j^* - 1\}$ where dispatch alterations are performed during a certain time step in a DR event. For example, when P_{req} is required by the system operator as shown in Fig. 5 (represented with a red solid line), the appliances in $\mathcal{X}_1$ and $\mathcal{X}_2$ only need to be controlled, where $\mathcal{X}_2$ will be the marginal cluster. Likewise, the emulated supply curve is used to determine the marginal cluster $\mathcal{X}_{j^*}$ and the lower priority clusters to be controlled to achieve P_{req} at a certain time.

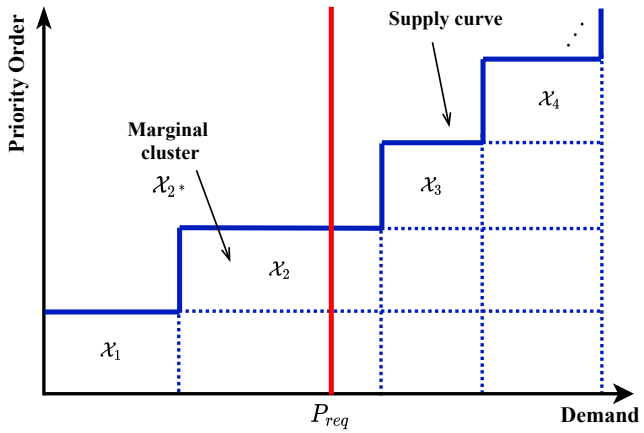

Fig. 5. Supply curve formation and the decision of marginal cluster

3.2. Optimisation problem

Once the marginal cluster $\mathcal{X}_{j^*}$ is determined from the supply curve as in section 3.1, the next step is to send control set-points: $\mathbf{P}_{\text{ref}}^{\text{AC}}$, $\mathbf{P}_{\text{ref}}^{\text{EWH}}$ to ACs and EWHs in that particular cluster as in Fig. 3. The DR controller achieves this by solving a one-step-ahead optimisation problem to determine the optimal selection of appliances to be controlled in $\mathcal{X}_{j^*}$ for the next time step. From the point of view of the aggregator, the objectives are to minimise the cost of buying electricity from wholesale markets or contracts, and to minimise discomfort for the contracted end customers. Therefore, a multi-objective optimisation problem is formed with the cost function to be a combination of total cost for the aggregator and the total discomfort for end customers. Considering $\mathcal{X}_{j^*}$ at time t, it can be expressed as,

$$F = w_{\text{cost}} \cdot \sum_i C_{p,t} \cdot (P_{i,t} - \Delta P_{i,t}) \cdot t_s + w_{\text{dis}} \cdot \sum_i DI_{i,t}^2 \quad \forall\, i \in \mathcal{X}_{j^*} \tag{9}$$

where $C_{p,t}$ is the market price of electricity at time t, $\Delta P_{i,t}$ is the power reduction and $CI_{i,t}$ is the discomfort index of appliance i at time t. In addition to that w_{cost} and w_{dis} represents the weights assigned to the cost and discomfort, respectively.

The discomfort index (DI) for ACs and EWHs at time t is obtained from [10] and mathematically expressed as,

$$DI_{i,t} = \frac{2\,T_{i,t}^x - \underline{T}_i^x - \overline{T}_i^x}{\overline{T}_i^x - \underline{T}_i^x} \quad \forall\, i \in \mathcal{A} \tag{10}$$

where $x = \{\text{room, outlet}\}$ s.t. $x = \text{room}$ for $i \in \Omega_{\text{AC}}$ and $x = \text{outlet}$ for $i \in \Omega_{\text{EWH}}$.

For $i \in \mathcal{X}_{j^*}$ at time t, the overall optimisation problem with constraints can be expressed as,

$$\underset{\Delta P^{AC}_{i,t}, \Delta P^{\text{EWH}}_{i,t}}{\text{minimise}} \quad F(\cdot) \tag{11}$$

$$\sum_i \Delta P^{\text{AC}}_{i,t} + \sum_i \Delta P^{\text{EWH}}_{i,t} \leq \overline{P}_{\text{req},t} \tag{12}$$

$$\underline{P}^{\text{AC}}_i \leq P^{\text{AC}}_{i,t} \leq \overline{P}^{\text{AC}}_i \tag{13}$$

$$\underline{P}^{\text{EWH}}_i \leq P^{\text{EWH}}_{i,t} \leq \overline{P}^{\text{EWH}}_i \tag{14}$$

$$P^{\text{AC}}_{i,t} = K^{\text{AC}}_{i,t} \cdot P^{\text{AC}}_{i,\text{rated}} \tag{15}$$

$$P^{\text{EWH}}_{i,t} = K^{\text{EWH}}_{i,t} \cdot P^{\text{EWH}}_{i,\text{rated}} \tag{16}$$

$$K^{\text{AC}}_{i,t}, K^{\text{EWH}}_{i,t} \in \mathcal{S} := \{0.25,\ 0.50,\ 0.75,\ 1.0\} \tag{17}$$

$$w_{\text{cost}} + w_{\text{dis}} = 1 \tag{18}$$

$$\text{s.t. } (2) - (7),\ (9),\ (10)$$

The constraint (12) corresponds to the minimum demand reduction required from the marginal priority cluster at time t. The constraints (13) and (14) describes the power limits for ACs and EWHs in the marginal priority cluster. The constraints (15), (16) and (17) describe the discrete power levels each AC and EWH can take. It is important to mention here that the minimum allowable consumption of an AC or EWH according to (17) is 0.25 times the rated power which is $P^{\text{AC/EWH}}_{\text{i,rated}}$ for $i \in \mathcal{X}_{j^*}$. Moreover, the values of $K^{\text{AC}}_{i,t}$ and $K^{\text{EWH}}_{i,t}$ in (17) are consistent with existing standards [49]. In addition to that, each objective term of the optimisation problem is normalised and the weights are assigned as in (18).

Remark 1. It is important to highlight that, despite solving a large-scale optimisation problem, i.e., a problem with $N_h \cdot n_a$ decision variables which will determine control set-points for ACs and EWHs at a particular time instant, the marginal cluster-based approach significantly simplifies the overall control problem. To elaborate this, control decisions have to be made only for N_h appliances in the marginal cluster $\mathcal{X}_{j^*}$ based on one-step-ahead optimisation whereas for appliances in non-marginal clusters $\{\mathcal{X}_1, \ldots, \mathcal{X}_{j^*-1}\}$, the control decision is trivial and does not require solving an optimisation problem.

The optimisation problem described by (11)-(18) represents a multi-objective mixed integer quadratic programming problem (MIQP) that consists N_h real decision variables $\{\Delta P^{AC}_{i,t}, \Delta P^{EWH}_{i,t}\}\ \forall\, i, \in \mathcal{X}_{j^*}$, N_h inequality constraints (12); N_h

bounding constraints representing (13) and (14); $2N_h + 1$ equality constraints from thermal dynamics represented by (4), (7) and multi-objective weights constraints given by (18), and N_h integral constraints due to (15), (16) and (17).

Let N be the set of appliances participating in the event. At time t, the mismatch between the desired reduction and the actual reduction can be expressed as,

$$e(t) = \overline{P}_{\text{req},t} - \sum_{i=1}^{N} \Delta P_{i,t} \qquad \forall\, i \in \mathcal{X}_{j^*} \tag{19}$$

Remark 2. It may be noted that $e(t)$ diminishes with increasing values of N. In fact, it can be proven that for a given $t \in [\,0\,, T_{\text{dur}}\,]$, as $N \longrightarrow \infty$, $\sum_i \Delta P_{i,t} \longrightarrow \overline{P}_{\text{req},t}$. This can be proven as follows:

$$\begin{aligned} e(t) &= \overline{P}_{\text{req},t} - \sum_{i=1}^{N} \Delta P_{i,t} \\ \text{however}\,, \quad \Delta P_{i,t} &= P_{i,t-1} - P_{i,t} \end{aligned}$$

Considering discrete levels from (15) and (16),

$$\begin{aligned} P_{i,t-1} &= \alpha_{i,t-1} \cdot P_{i,\text{rated}} \\ P_{i,t} &= \alpha_{i,t} \cdot P_{i,\text{rated}} \\ \therefore\ e(t) &= \overline{P}_{\text{req},t} - \sum_{i=1}^{N} (\alpha_{i,t-1} - \alpha_{i,t}) \cdot P_{i,\text{rated}} \end{aligned}$$

Since $\Delta P_{i,t} \geq 0$, $(\alpha_{i,t-1} - \alpha_{i,t}) \geq 0\, \forall\, i, t$ and $P_{i,\text{rated}} \geq 0\, \forall\, i$. Therefore, $N \longrightarrow \infty$ results in $\| \sum_{i=1}^{N} (\alpha_{i,t-1} - \alpha_{i,t}) \cdot P_{i,\text{rated}} \| \longrightarrow | \sum_{i=1}^{N} (\alpha_{i,t-1} - \alpha_{i,t}) \cdot P_{i,\text{rated}} |_{\max} = \overline{P}_{\text{req},t}$ obtained from (12). This proves that for a given $t \in [\,0\,, T_{\text{dur}}\,]$, as $N \longrightarrow \infty$, $\|e(t)\| \longrightarrow 0$ and $\sum_i \Delta P_{i,t} \longrightarrow \overline{P}_{\text{req},t}$.

It is also worth mentioning that, although this work focuses only on controlling comfort-based elastic devices [61, 62] such as air conditioners and water heaters, the approach could be extended to control energy-based elastic devices by utilising proper mathematical models as in [61] and designing an index to quantify discomfort when controlled (similar to (10)). Thereafter, an optimisation problem similar to (11)-(18) could be formulated with additional constraints for energy-based control devices to determine control set-points for the pool of comfort-based and energy-based controllable devices in the marginal cluster.

3.3. Implementation

After determining the ACs and EWHs to be controlled in the marginal cluster and lower priority clusters based on the emulated supply curve in section 3.1 and one-step-ahead optimisation in section 3.2, the DR controller sends control commands to obtain desired demand reduction at a certain time step. Since the DR controller only has access to real-time power consumption measurements but not temperature measurements, the output power consumption measurements are used to estimate indoor temperature for ACs and outlet temperature for EWHs with the help of thermal models (4) and (7) as shown in Fig. 3. After that, with updated power consumption measurements, the DR controller estimates the actual demand reduction ($P_{\text{act},t}$) and compares it with the reference power reduction ($P_{\text{req},t}$). Thereafter, additional control commands are deployed at next step to account for mismatches in demand reduction resulting from uncertainties.

3.4. Operation under system uncertainties

If perfect control operation is assumed, determining control set-points in terms of $\Delta P_{i,t}^{\text{AC}}$ and $\Delta P_{i,t}^{\text{EWH}}$ for $i \in \{\mathcal{X}_1, \ldots, \mathcal{X}_{j^*}\}, \forall t$ would be sufficient for the DR controller. However, in reality, due to uncertainties that can occur at any time, for example, deviations of actual consumption from the reference set-point, i.e., $\mathbf{P}_{\text{out}}^{\text{AC/EWH}} \neq \mathbf{P}_{\text{ref}}^{\text{AC/EWH}}$; changes in P_{req}; the DR controller will not be able to deliver desired demand reductions as expected. Hence, an algorithm is developed to achieve precise load reduction under the following uncertainties arising in real-time operation:

- Customer non-compliance events at a particular time during the DR event.
- Violation of temperature limits during a DR event.
- A change in the set point reduction at a particular time instant during the DR event.

In addition to that, an approach identical to 'meter-before-meter-after' method [63] is utilised to determine the actual demand reduction $P_{act,t}$, for $t > 0$. Considering time t, this can be expressed as:

$$P_{act,t} = \sum_i (P_{i,0}^{\text{AC}} - P_{i,t}^{\text{AC}}) + \sum_i (P_{i,0}^{\text{EWH}} - P_{i,t}^{\text{EWH}}) \tag{20}$$

where $P_{i,0}^{\text{AC}}$ and $P_{i,0}^{\text{EWH}}$ are the initial power consumption of i^{th} air conditioner and i^{th} water heater. The overall operation under uncertainties is described in Algorithm 1.

3.4.1. A customer override event

A customer override event, i.e., an end-user non-compliance event, refers to a scenario where a customer interrupts the aggregator sent DR signal to alter the operational state of an appliance. In terms of the nomenclature introduced in this work, the indication of a customer override event for the i^{th} AC at time t is given by $\psi_{i,t}^{\text{AC}} = 1$. Following an override event at time t, the actual demand reduction deviates from the desired reduction, i.e. $P_{\text{act},t} < P_{\text{req},t}$. Hence, additional units are dispatched at time $t + 1$ to compensate for the mismatch. The expected demand reduction at time $t + 1$ following an override event at time t can be expressed as, $P_{\text{req},t+1} = P_{\text{req},t} - P_{\text{act},t}$.

Let the set of appliances overridden at time t is denoted by $O_t = \{ i \in \mathcal{A} \mid \psi_{i,t} = 1\}$. With the DR policy considered in this paper, the appliances in O_t are opted-out and not controlled for the rest of the DR event. In addition to that, the supply curve is only formed with the flexible consumption of units which have not encountered voluntary compliance. The lines 24 and 32 in Algorithm 1 corresponds to checking whether an override event has occurred at a certain time instant.

3.4.2. Uncertainty arising due to temperature limit violations

The appliance selection for the DR in this work depends on the combination of supply curve formulation and solving a one-step-ahead optimisation problem. However, there is no guarantee that temperature for ACs and EWHs will remain within the preferred limits at each time step during the DR event. Hence, the lines 7 to 21 in Algorithm 1 takes into account the uncertainties due to temperature violations. Once appliances are controlled to achieve the desired reduction at a certain time step, the corresponding room temperature for ACs and the outlet temperature for EWHs are calculated for the next time step with (4) and (7) and compared with their corresponding bounds ($\overline{T}^{\text{room}}$ for ACs and $\underline{T}^{\text{outlet}}$ for EWHs). If the temperature for the next step violates the comfort limits, the control over the appliance is released.

3.4.3. Set point change event

This corresponds to a change in the demand reduction signal sent by the system operator. Usually, a set-point change could be either an increase or decrease in P_{req}. However, this work only considers an increase in set point where additional demand reduction needs to be achieved at a certain time step. Similar to a customer override event, set point change could occur at any time in a DR event. Hence, at each time step Algorithm 1 checks for a change in set-point (lines 25,

Algorithm 1: The operation of the DR controller under uncertainties

Initialise $t = 0$;
Input: P_{req}, T_{dur}, $P_{i,0}^{\text{AC}}$, $P_{i,0}^{\text{EWH}}$, $\overline{T}_i^{\text{room}}$, $\underline{T}_i^{\text{outlet}}$, priority index j, modelling parameters for all i ;
Determine t_s based on T_{dur} and the type of event;
Supply curve formation to determine $\mathcal{X}_{j^*}$;
Optimisation process to dispatch appliances in $\mathcal{X}_{j^*}$;
for $t = 1;\ t \leq T_{\text{dur}}$ **do**
    Calculate $T_{i,t}^{\text{room}}$ with (4) ;
    Calculate $T_{i,t}^{\text{outlet}}$ with (7) ;
    for $i \in \Omega_{\text{AC}}$ **do**
        if $T_{i,t}^{\text{room}} > \overline{T}_i^{\text{room}}$ **then**
            Update $P_{i,t}^{\text{AC}} = P_{i,\text{rated}}^{\text{AC}}$;
        else
            Keep $P_{i,t}^{\text{AC}}$;
        end
    end
    for $i \in \Omega_{\text{EWH}}$ **do**
        if $T_{i,t}^{\text{outlet}} < \underline{T}_i^{\text{outlet}}$ **then**
            Update $P_{i,t}^{\text{EWH}} = P_{i,\text{rated}}^{\text{EWH}}$;
        else
            Keep $P_{i,t}^{\text{EWH}}$;
        end
    end
    Calculate $P_{\text{act},t}$ as in (20) ;
    if $P_{\text{req},t} < P_{\text{req},t}$ **then**
        if $P_{\text{req},t+1} > P_{\text{req},t}$ **then**
            Update $P_{\text{req},t+1} = (P_{\text{req},t+1} - P_{\text{req},t}) + (P_{\text{req},t} - P_{\text{act},t})$;
        if $P_{\text{req},t+1} = P_{\text{req},t}$ **then**
            Update $P_{\text{req},t+1} = P_{\text{req},t} - P_{\text{act},t}$;
        end
        Determine O_t with (1) ;
        Avoid sending control signals $\forall\, i \in O_t$ for $t \in [\,t+1, T_{\text{dur}}\,]$;
    if $P_{\text{act},t} \geq P_{\text{req},t}$ **then**
        if $P_{\text{req},t+1} > P_{\text{req},t}$ **then**
            Update $P_{\text{req},t+1} = P_{\text{req},t+1} - P_{\text{req},t}$;
        if $P_{\text{req},t+1} = P_{\text{req},t}$ **then**
            Update $P_{\text{req},t+1} = 0$;
        end
    end
    Supply curve formation to determine $\mathcal{X}_{j^*}$ based on $P_{\text{req},t+1}$;
    Optimisation process to dispatch appliances in $\mathcal{X}_{j^*}$;
end

27, 33 and 35) and determines the additional demand reduction required in the subsequent step.

Considering the overall process, Algorithm 1 first determines temperature violations at each step and implements necessary control actions. Thereafter, it checks for customer override events and set-point changes simultaneously at each time step and determines the additional demand reduction based on their occurrences. Once the additional demand reduction is determined, supply curve formulation and one-step-ahead optimisation is performed to deploy control commands on a chosen set of appliances. This process is repeated until the end of the DR event.

A low-level control diagram providing information on the overall closed-loop implementation is given in Fig. 6.

4. Results and Discussions

The proposed DR approach is implemented on two sets of population schemes such that $N_h = 100$ and $N_h = 1000$ in which customers have contracts with an aggregator to control the consumption of ACs and EWHs.

Consistent with the proposed approach, it is assumed that the underlying infrastructure is present for the end-users to communicate with the DR controller. The sampling period t_s is considered to be 1-min to align with present and future dispatch intervals of the National Electricity Market (NEM) [65] under the participation of residential DR. The effect of delays and imperfections in the communication link is assumed to be minimal due to the sufficiently long sampling period. Furthermore, the operation of residential ACs and EWHs are assumed to be in compliance with demand response standards described in [49].

The priority j for AC and EWH at each house is randomly generated. Hence, the supply curve in Fig. 5 is formed with clusters $\mathcal{X}_1$ and $\mathcal{X}_2$. However, this approach can be further extended to include more clusters in the supply curve, if customers allow their electric vehicles (EVs), pool pumps to be controlled.

For the AC subsystem, the real-time power consumption data is obtained from [46]. The outdoor temperature profile is obtained from [66] and given in Fig. 7. Further, $\underline{T}^{\text{room}}$ and $\overline{T}^{\text{room}}$ for ACs are assumed to vary uniformly as $\mathcal{U}(68, 71.6)$°F $\approx \mathcal{U}(20, 22)$°C, and $\mathcal{U}(78.8, 80.6)$°F $\approx \mathcal{U}(26, 27)$°C, where $\mathcal{U}(.)$ is a uniform distribution. At the beginning of the DR event, it is assumed that all ACs are operating at their set point $\mathcal{U}(71.6, 75.2)$°F $\approx \mathcal{U}(22, 24)$°C. Then (4) is used to determine the rated consumption of ACs and to generate reconstructed power

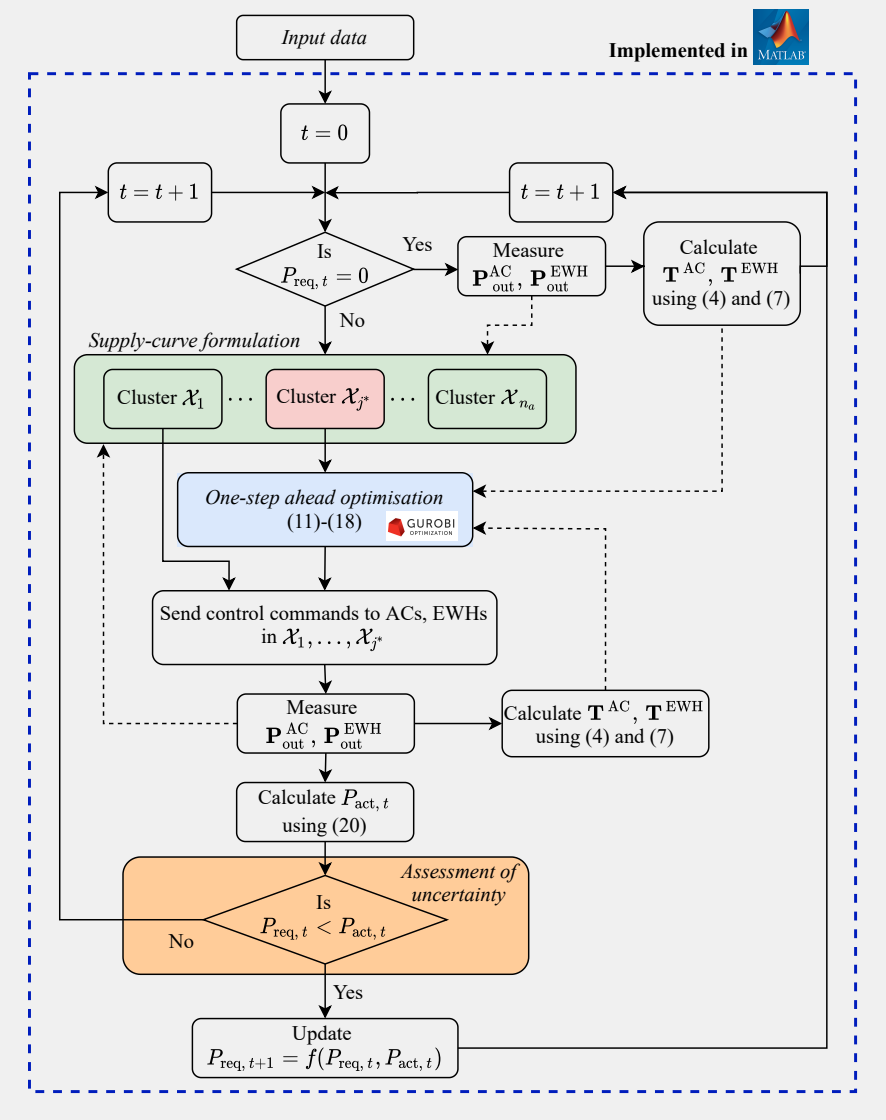

Fig. 6. A low-level control diagram illustrating the overall closed-loop implementation; control algorithms are implemented in MATLAB R2019a and *Gurobi 9.0.2* [64] is used to solve the one-step ahead optimisation problem; solid lines represent control flow and dashed lines represent information flow

consumption profiles based on the data set. This procedure is followed to make sure that all ACs are operating at their rated consumption before the DR event.

For the EWH subsystem, it is assumed that T^{inlet} and T^{amb} are constant. $\underline{T}^{\text{outlet}}$

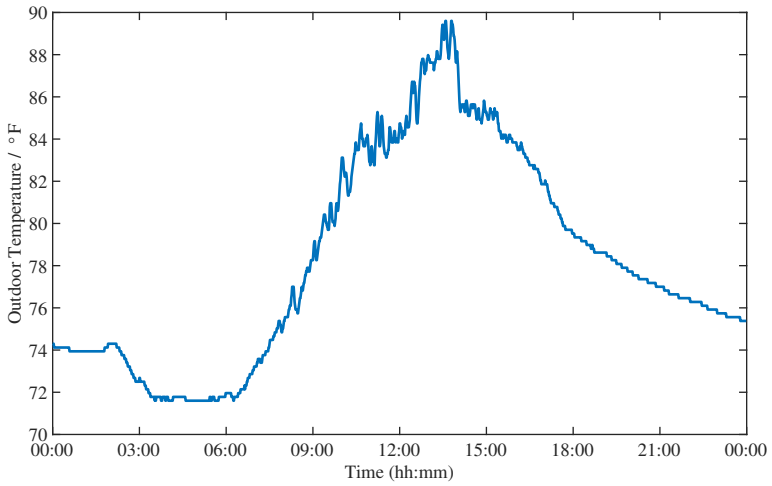

Fig. 7. Outdoor temperature on 22-03-2020 obtained from [66]

is assumed $\mathcal{U}(120, 125)$°F and $\overline{T}^{\text{outlet}}$ is assumed $\mathcal{U}(160, 165)$°F. Moreover, the EWHS are operating at their set point $\mathcal{U}(140, 150)$°F before the DR event. Furthermore, it is assumed that the f^r is uniformly distributed and remains constant during the DR interval. Similar to ACs, the rated consumption for EWHs are calculated from (7) to generate reconstructed profiles based on actual consumption data obtained from [46]. Following this, it is guaranteed that all EWHs are operating at their set point under rated consumption before the DR event. Under normal conditions, a EWH usually operates at rated consumption for around 1 hour to restore a fully empty tank with heated water. For longer DR events, the above assumption is not reasonable.

It is important to highlight that the dataset for the trials conducted by [46] is not publicly available. However, for the sake of completion, Fig. 8 illustrates sample power consumption profiles for ACs and EWHs obtained from [46]. It is evident from Fig. 8 that inverter-type air conditioners operate under continuous power levels unlike regular ON-OFF type air conditioners where the power consumption periodically varies between zero and rated power. Moving on to EWH profiles, it can be clearly observed the normal operation under rated power is only limited to shorter durations (less than 1 hour).

Aligned with the typical behaviour of inverter-type ACs and EWHs, a demand reduction event is considered for $T_{\text{dur}} = 1$ hour, starting from 15:00 and ending at 16:00 on 22-03-2020. The market price of electricity $C_{p,t}$ is assumed constant and obtained from [65].

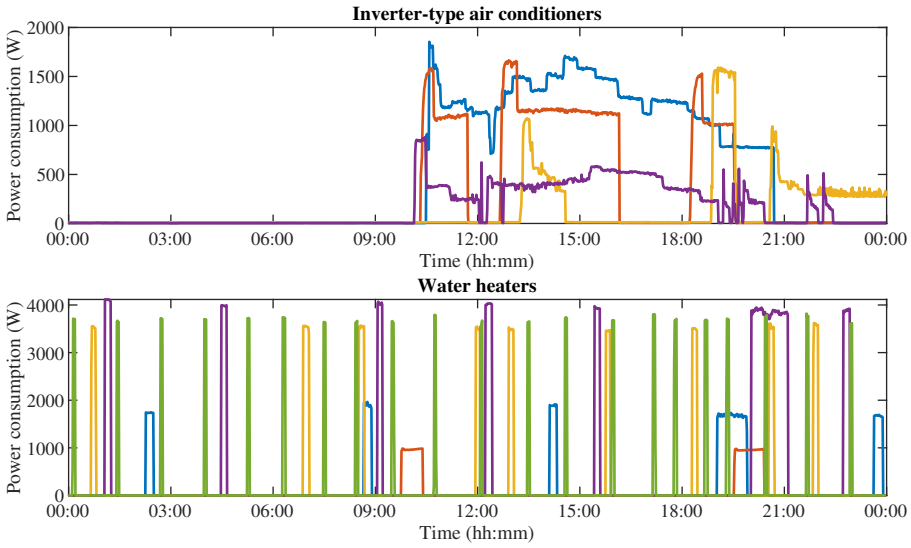

Fig. 8. Sample power consumption profiles for inverter-type air conditioners and electric storage-type water heaters obtained from [46] (1-min resolution)

As illustrated in Fig. 6, all the control algorithms: marginal cluster determination; operation under uncertainties (Algorithm 1); are written in MATLAB 2019a. The one-step ahead optimisation problem (MIQP problem) described by (11)-(18) is also modelled in MATLAB 2019a together with *YALMIP* toolbox [67] and solved using *Gurobi 9.0.2* [64]. The simulations are performed on a computer equipped with an Intel(R) Xeon(R) CPU E5-2680 v3 @ 2.50 GHz and 32 GB RAM memory.

In addition to determining the effect of population size N_h on the actual demand reduction, the proposed approach under pre-defined levels of consumption is compared with a non-explicit approach where ACs and EWHs are capable of operating at any non-standard (non-discrete) consumption level between 25% and 100% of the rated power.

Fig. 9 illustrates such a simulated scenario (similar to [68]) where ACs and EWHs in a certain cluster together provide 100 kW of demand reduction assuming no uncertainties exist during the control period. As can be seen from temperature plots, at the end of the control period, indoor temperature reaches 80°F ≈ 26.6°C for certain air conditioners; the outlet temperature reaches as low as 100°F ≈ 37.7°C for certain water heaters; which is undesirable. Nonetheless, some devices operate at nominal temperature throughout the event. This would ultimately lead

to customer non-compliance events due to the compromise of thermal comfort of affected end-users. Hence, it is clear that such an uneven control approach is not desirable in a practical setting where uncertainties can no longer be ignored.

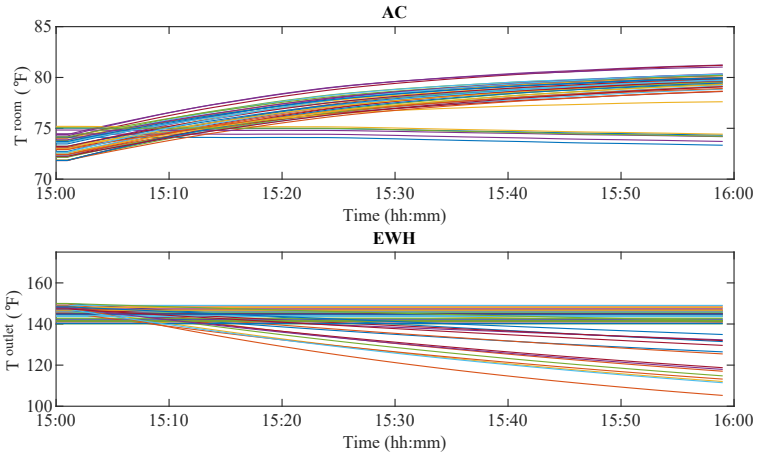

Fig. 9. The variation of T^{room} for ACs and T^{outlet} for EWHs in a certain cluster when obtaining 100 kW with $N_h = 100$ under no uncertainties in the overall system

4.1. Performance under the influence of uncertainties

Simulations are performed mainly for two scenarios: 1) a set of customers override the control signals sent by the aggregator during the DR event; 2) the aggregator decides to increase the target reduction during a DR event. While achieving the desired demand reduction under above uncertainties, temperature violations are also taken into account.

4.1.1. Customer non-compliance event

In the actual implementation, the non-compliance action is only realisable with air conditioners [49]. Once the customer overrides the DR event, the control action is released and the AC continues to operate at the rated consumption for the rest of the DR event. While the aggregator is delivering 100 kW, it is simulated that 20% of the ACs in cluster $\mathcal{X}_1$ override the control action at 15:10.

Fig. 10 shows the performance of the control scheme in acquiring 100 kW with N_h=100 and N_h=1000. The dip in the actual reduction profile at 15:10 for both the discrete and non-discrete scenarios correspond to 20% overriding action in $\mathcal{X}_1$. After the overriding event, additional units are dispatched for compensation and to follow the desired reduction at 15:11. Thereafter, for the rest of the

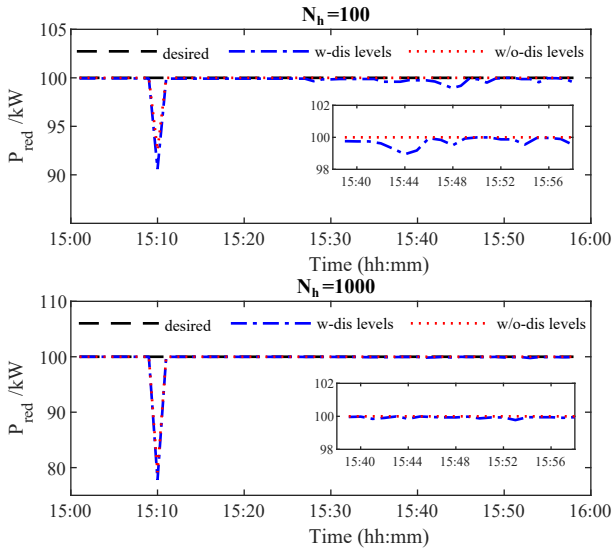

Fig. 10. Comparison of demand reduction under customer override for $N_h = 100$ and $N_h = 1000$

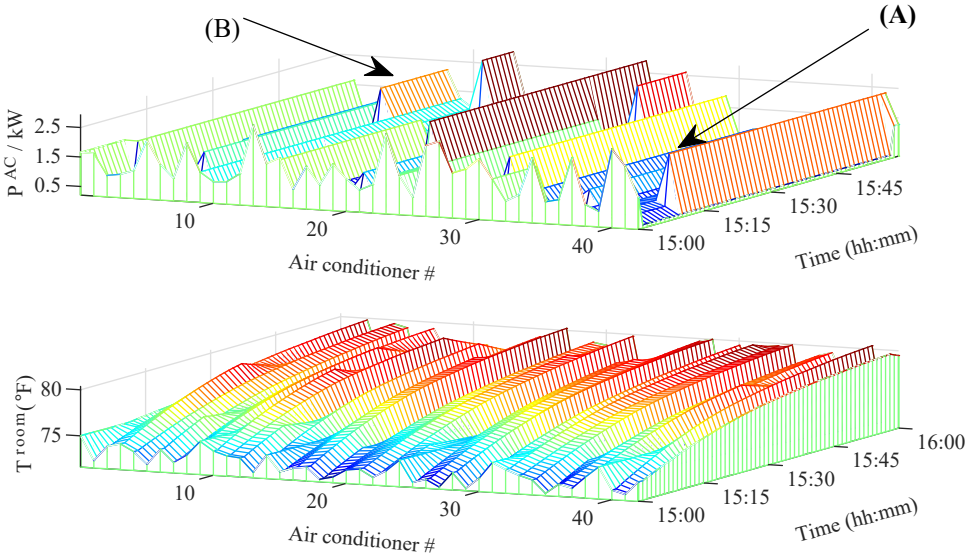

Fig. 11. The variation of P^{AC} and T^{room} for a customer override event with $N_h = 100$: (A) represents an override event for a certain AC; (B) represents an event where an AC resumes the operation at rated power due to temperature violations

DR event, the control scheme follows the targeted reduction while mitigating demand reduction mismatches due to the release of control on appliances once they reach their temperature limits. For N_h=100, it is observed that the proposed discrete level implementation achieves the performance of the non-standard scheme with small deviations in the actual reduction profile. However, for N_h=1000, it is identified that the proposed scheme is identical to the non-discrete scheme and achieves perfect tracking.

Fig. 11 illustrates the corresponding variation of power consumption and temperature of ACs in $\mathcal{X}_1$ for a population of N_h=100 under the override control action. After operating at de-rated condition until 15:10, some air conditioners override the control action and resume the operation at rated power. This is clearly seen in the power consumption profile of ACs at 15:10. Based on the DR policy followed in this work, they remain operating at rated power until the DR event ends at 16:00. On the other hand, for ACs that do not undergo non-compliance, temperatures reach their upper thermal limits midway during the control period. Consequently, the DR controller avoids temperature violations according to Algorithm 1 by eliminating the control action on affected units and allowing them to operate at rated consumption. This is clearly seen in the power consumption profile around 15:30 where some ACs suddenly start to operate at rated power. Since this would lead to a mismatch in the desired demand reduction, the DR controller decides to deploy additional control actions on ACs based on (11)-(18) for the next sampling instant. This back-and-forth temperature violations and demand mismatch correction process results in pulses in the power consumption profile and fluctuations in the temperature profile towards the end of the DR event. However, at the end, the overall control scheme is capable of providing desired demand reduction while controlling temperature within preferred limits (probably < 80°F) as observed in the overall indoor temperature profile.

4.1.2. Change in the set point

As shown in Fig. 12, simulations are performed for a scenario where the system operator decides to increase the set-point from 75 kW to 125 kW at time 15:10. From 15:00 until 15:10, the aggregator perfectly follows the set-point by delivering 75 kW of demand reduction. Following the system operator's command at 15:10, the aggregator executes Algorithm 1 to send alternate dispatch signals to compensate for the unmatched 50 kW demand reduction. Thereafter, the aggregator delivers 125 kW of demand reduction until the end of the event. The inconsistent tracking around 15:52 for $N_h = 100$ is due to the limited flexibility to obtain 125 kW with $N_h = 100$ when the control action is released after

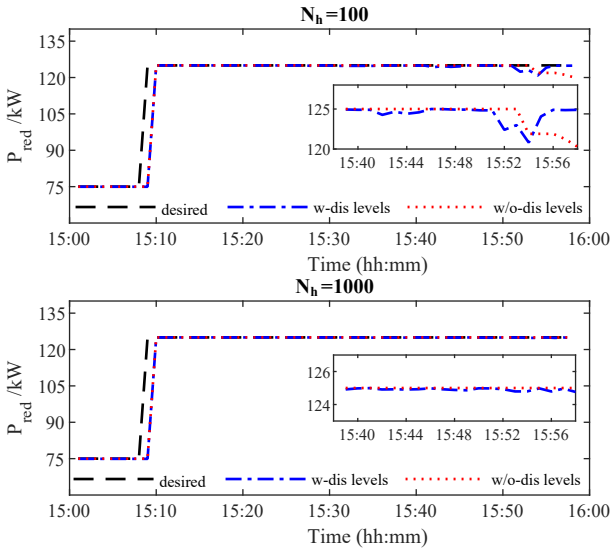

Fig. 12. Comparison of demand reduction under a set point change event for $N_h = 100$ and $N_h = 1000$

appliances reach their temperature limits. However, this inconsistent behaviour is eliminated and perfect tracking is achieved when $N_h = 1000$ is considered. Thus, the proposed control scheme is capable of providing effective and timely response to a change in load set-point signal commanded by the system operator without compromising temperature comfort of participating end-users.

4.1.3. Comparison of total execution time

The total execution time, i.e. the time taken to implement control actions for T_{dur}, is compared for the uncertainty scenarios: customer override and set-point changes, under different population sizes N_h, with and without discrete consumption levels for ACs and EWHs. The results are summarised in Table 3.

As can be seen from Table 3, the operation under discrete consumption levels is more computationally expensive compared to the operation under non-discrete consumption levels for the same N_h under the same uncertainty scenario. This is expected as the approach under discrete consumption levels involves solving a one-step ahead optimisation problem which is MIQP in nature. However, no significant variation in total execution time is observed when the operation under a customer override event and a set-point change event are compared. Nonetheless, the total execution time remains within the allowable $T_{dur} = 1\,\text{hr} = 3600\,\text{sec}$ limit

Table 3. Comparison of total execution time for uncertainty events under different population sizes N_h

Number of houses (N_h)	Total execution time (sec)			
	customer override		*set-point change*	
	without-discrete	with-discrete	without-discrete	with-discrete
100	55.22	142.8	14.52	213.5
1000	188.6	2857	176.0	2823

– simulations are performed on a computer equipped with an Intel(R) Xeon(R) CPU E5-2680 v3 @ 2.5GHz 32 GB RAM memory.

for all the scenarios considered. Hence, it can be argued that the proposed control scheme is computationally tractable and is applicable for practical implementation under large scale aggregation of consumer-owned TCLs.

4.2. Comparison with a current industrial practice

One of the existing approaches is *PeakSmart* [69], a commercial DR scheme in Queensland, Australia. As per their practice, the retailer or the DR aggregator broadcasts an identical control signal, e.g., 25% of rated consumption, irrespective of operating conditions, to all participating customers during a demand response event. On the other hand, the approach proposed in this work follows a systematic method: supply-curve based cluster selection and one-step-ahead optimisation, to send different control set-points, e.g., 25%, 50%, 75%, 100% of rated power, only to a limited set of appliances. Despite the effort made to control inverter-type air conditioners, the existing method [69] also lacks control capabilities to handle uncertainties, for instance, customer override capabilities, which makes it unsuitable for the provision of grid services where perfect tracking of the load set-point signal is essential to avoid financial penalties.

Fig. 13 gives information on a comparison between the existing approach [69] and our method when achieving 25% demand reduction only from inverter-type ACs. Based on the assumption that the control is only limited to ACs and EWHs, the supply-curve is formulated with two clusters: $\mathcal{X}_1$, $\mathcal{X}_2$ and the control action occurs only in $\mathcal{X}_1$ (marginal cluster). Further investigation of the temperature profile yields that indoor temperature for ACs in $\mathcal{X}_1$ reach upper thermal limits towards the end of the DR event whereas temperatures remain almost unchanged for ACs in $\mathcal{X}_2$. By this manner, the proposed approach provides 25% of demand reduction.

Since identical control set-points are sent to all the participating devices in the existing approach, it is observed that indoor temperature deviates from set-point for most of the air conditioners. However, the level of thermal discomfort experienced by end-users is identified to be lower than in our approach where ACs only in $\mathcal{X}_1$ are controlled. This can be understood by the distributed nature of the control action in the existing approach which does not require a portion of the units to be controlled with a higher effort, rather requires the entire population to be controlled with same effort. Nonetheless, it is worth noting that there is always a trade-off between the cost of control (depends on the number of ACs controlled) and the level of thermal comfort experienced.

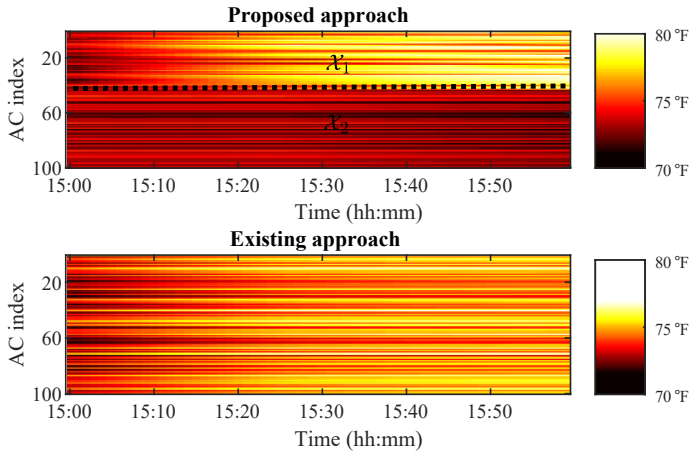

Fig. 13. The variation of room temperature under the proposed approach and the existing approach [69] while achieving 25% demand reduction from $N_h = 100$

5. Conclusion

This paper presents a control approach using residential controllable loads to provide desired demand reduction whilst taking into account the uncertain factors that are inevitable in practice. The uncertain factors that are considered include end-user non-compliance action, end-user thermal comfort violations, and changes in the load set-point. A two-stage approach embedded with uncertainty handling capabilities is proposed. The first stage is to determine priority clusters to be controlled via an emulated supply curve formed by grouping appliances based on end-user assigned priority levels. This is followed by solving a one-step-ahead optimisation problem to determine the optimal control of devices within

the chosen priority clusters. Simulations are validated using a real data set for inverter-type air conditioners and electric water heaters on two population sizes under explicit discrete level control aligned with existing demand response standards and non-explicit consideration of standard levels.

Some of the key insights gained from the study are as follows:

- The same level of performance of a non-explicit control scheme can be achieved even with the consideration of discrete power consumption levels in the presence of uncertainties.
- The tracking performance of the proposed control scheme increases as the population size of the controllable loads increases.
- Through effective uncertainty mitigation, the proposed control scheme has the potential to outperform existing commercial implementations in terms of accurate tracking capabilities and reduced control effort requirement.

The findings of this study will be of importance to retailers or demand response aggregators to devise control schemes to mitigate financial penalties and to maximise social welfare in future electricity markets where active end-user participation is prevalent.

The future work will be to enhance the performance of the developed control scheme against latency and other imperfections in the bi-directional communication infrastructure.

Acknowledgment

The authors would like to thank for the support given by the Centre for Energy Data Innovation (CEDI), The University of Queensland, under the Advance Queensland grant (grant no: AQPTP01216-17RD1).

Appendix A. Thermal parameters for AC and EWH models

Table A.4. Parameters of residential air conditioning systems [55]

Parameter	Description	Unit
h	height of the ceiling	ft
A^{floor}	area of the floor	ft^2
A^{wall}	area of the walls	ft^2
A^{ceil}	area of the ceiling	ft^2
A^{win}	area of the windows	ft^2
A^{sw}	area of the south-windows	ft^2
V^h	volume of the house	ft^3
R^{wall}	thermal resistance of walls	$^\circ\text{F} \cdot \text{ft}^2 \cdot \text{h}/\text{Btu}$
R^{ceil}	thermal resistance of the ceiling	$^\circ\text{F} \cdot \text{ft}^2 \cdot \text{h}/\text{Btu}$
R^{win}	thermal resistance of windows	$^\circ\text{F} \cdot \text{ft}^2 \cdot \text{h}/\text{Btu}$
η_{ac}	number of air changes	(1/h)
SHGC	solar heat gain coefficient of windows	—
H^s	solar radiation of heat power	W/m^2
H^p	heat gain from people	Btu/h

Table A.5. Parameters of residential water heating systems [55]

Parameter	Description	Unit
V^{tank}	volume of the tank	gal
A^{tank}	area of the tank	ft^2
R^{tank}	thermal resistance of the tank	$^\circ\text{F} \cdot \text{ft}^2 \cdot \text{h}/\text{Btu}$
f^r	flow rate	gal/min
T^{inlet}	Inlet temperature of water	°F

References

[1] International Renewable Energy Agency (IRENA), Solutions to integrate high shares of variable renewable energy, https://www.irena.org/-/media/Files/IRENA/Agency/%20Publication/2019/Jun/IRENA_G20_grid_integration_2019.pdf, Accessed: 12-01-2020.

[2] D. S. Callaway, I. A. Hiskens, Achieving Controllability of Electric Loads, Proceedings of the IEEE 99 (1) (2011) 184–199. doi:10.1109/JPROC.2010.2081652.

[3] J. S. Vardakas, N. Zorba, C. V. Verikoukis, A Survey on Demand Response Programs in Smart Grids: Pricing Methods and Optimization Algorithms, IEEE Communications Surveys Tutorials 17 (1) (2015) 152–178. doi:10.1109/COMST.2014.2341586.

[4] P. Siano, Demand response and smart grids—A survey, Renewable and Sustainable Energy Reviews 30 (2014) 461–478. doi:https://doi.org/10.1016/j.rser.2013.10.022.

[5] R. Adhikari, M. Pipattanasomporn, S. Rahman, An algorithm for optimal management of aggregated HVAC power demand using smart thermostats, Applied Energy 217 (2018) 166–177. doi:https://doi.org/10.1016/j.apenergy.2018.02.085.

[6] W. Zhang, J. Lian, C. Y. Chang, K. Kalsi, Aggregated Modeling and Control of Air Conditioning Loads for Demand Response, IEEE Transactions on Power Systems 28 (4) (2013) 4655–4664. doi:10.1109/TPWRS.2013.2266121.

[7] J. L. Mathieu, S. Koch, D. S. Callaway, State Estimation and Control of Electric Loads to Manage Real-Time Energy Imbalance, IEEE Transactions on Power Systems 28 (1) (2013) 430–440. doi:10.1109/TPWRS.2012.2204074.

[8] S. Bashash, H. K. Fathy, Modeling and Control of Aggregate Air Conditioning Loads for Robust Renewable Power Management, IEEE Transactions on Control Systems Technology 21 (4) (2013) 1318–1327. doi:10.1109/TCST.2012.2204261.

[9] A. Taşcıkaraoğlu, N. G. Paterakis, O. Erdinç, J. P. S. Catalão, Combining the Flexibility From Shared Energy Storage Systems and DLC-Based Demand Response of HVAC Units for Distribution System Operation Enhancement, IEEE Transactions on Sustainable Energy 10 (1) (2019) 137–148. doi:10.1109/TSTE.2018.2828337.

[10] Q. Hu, F. Li, X. Fang, L. Bai, A Framework of Residential Demand Aggregation With Financial Incentives, IEEE Transactions on Smart Grid 9 (1) (2018) 497–505. doi:10.1109/TSG.2016.2631083.

[11] M. Pied, M. F. Anjos, R. P. Malhamé, A flexibility product for electric water heater aggregators on electricity markets, Applied Energy 280 (2020) 115168. doi:https://doi.org/10.1016/j.apenergy.2020.115168.

[12] M. Maasoumy, M. Razmara, M. Shahbakhti, A. S. Vincentelli, Handling model uncertainty in model predictive control for energy efficient buildings, Energy and Buildings 77 (2014) 377–392. doi:https://doi.org/10.1016/j.enbuild.2014.03.057.

[13] C. Lork, W.-T. Li, Y. Qin, Y. Zhou, C. Yuen, W. Tushar, T. K. Saha, An uncertainty-aware deep reinforcement learning framework for residential air conditioning energy management, Applied Energy 276 (2020) 115426. doi:https://doi.org/10.1016/j.apenergy.2020.115426.

[14] O. Erdinc, A. Tascikaraoglu, N. G. Paterakis, J. P. S. Catalao, Novel Incentive Mechanism for End-Users Enrolled in DLC-Based Demand Response Programs Within Stochastic Planning Context, IEEE Transactions on Industrial Electronics 66 (2) (2019) 1476–1487. doi:10.1109/TIE.2018.2811403.

[15] F. Oldewurtel, A. Parisio, C. N. Jones, D. Gyalistras, M. Gwerder, V. Stauch, B. Lehmann, M. Morari, Use of model predictive control and weather forecasts for energy efficient building climate control, Energy and Buildings 45 (2012) 15–27. doi:https://doi.org/10.1016/j.enbuild.2011.09.022.

[16] S. M. Hosseini, R. Carli, M. Dotoli, Robust Optimal Energy Management of a Residential Microgrid Under Uncertainties on Demand and Renewable Power Generation, IEEE Transactions on Automation Science and Engineering 18 (2) (2021) 618–637. doi:10.1109/TASE.2020.2986269.

[17] R. Shi, S. Li, P. Zhang, K. Y. Lee, Integration of renewable energy sources and electric vehicles in V2G network with adjustable robust optimization, Renewable Energy 153 (2020) 1067–1080. doi:https://doi.org/10.1016/j.renene.2020.02.027.

[18] S. Paul, N. P. Padhy, Resilient Scheduling Portfolio of Residential Devices and Plug-In Electric Vehicle by Minimizing Conditional Value at Risk, IEEE Transactions on Industrial Informatics 15 (3) (2019) 1566–1578. doi:10.1109/TII.2018.2847742.

[19] A. R. Jordehi, M. S. Javadi, J. P. S. Catalão, Day-ahead scheduling of energy hubs with parking lots for electric vehicles considering uncertainties, Energy 229 (2021) 120709. doi:https://doi.org/10.1016/j.energy.2021.120709.

[20] S. R. Konda, B. Mukkapati, L. K. Panwar, B. K. Panigrahi, R. Kumar, Dynamic Energy Balancing Cost Model for Day Ahead Markets with Uncertain Wind Energy and Generation Contingency under Demand Response, IEEE Transactions on Industry Applications 54 (5) (2018) 4908–4916. doi:10.1109/TIA.2018.2844363.

[21] K. Paridari, A. Parisio, H. Sandberg, K. H. Johansson, Robust Scheduling of Smart Appliances in Active Apartments With User Behavior Uncertainty, IEEE Transactions on Automation Science and Engineering 13 (1) (2016) 247–259. doi:10.1109/TASE.2015.2497300.

[22] F. Wang, X. Ge, P. Yang, K. Li, Z. Mi, P. Siano, N. Duić, Day-ahead optimal bidding and scheduling strategies for DER aggregator considering responsive uncertainty under real-time pricing, Energy 213 (2020) 118765. doi:https://doi.org/10.1016/j.energy.2020.118765.

[23] N. Good, E. Karangelos, A. Navarro-Espinosa, P. Mancarella, Optimization Under Uncertainty of Thermal Storage-Based Flexible Demand Response With Quantification of Residential Users' Discomfort, IEEE Transactions on Smart Grid 6 (5) (2015) 2333–2342. doi:10.1109/TSG.2015.2399974.

[24] M. J. Salehpour, S. M. Moghaddas Tafreshi, The effect of price responsive loads uncertainty on the risk-constrained optimal operation of a smart micro-grid, International Journal of Electrical Power and Energy Systems 106 (2019) 546–560. doi:10.1016/j.ijepes.2018.10.027.

[25] C. Wang, Y. Zhou, B. Jiao, Y. Wang, W. Liu, D. Wang, Robust optimization for load scheduling of a smart home with photovoltaic system, Energy Conversion and Management 102 (2015) 247–257. doi:https://doi.org/10.1016/j.enconman.2015.01.053.

[26] H. J. Kim, M. K. Kim, Risk-based hybrid energy management with developing bidding strategy and advanced demand response of grid-connected microgrid based on stochastic/information gap decision theory, International Journal of Electrical Power & Energy Systems 131 (2021) 107046. doi:https://doi.org/10.1016/j.ijepes.2021.107046.

[27] M. Vahedipour-Dahraie, H. Rashidizadeh-Kermani, M. Shafie-Khah, J. P. S. Catalão, Risk-Averse Optimal Energy and Reserve Scheduling for Virtual Power Plants Incorporating Demand Response Programs, IEEE Transactions on Smart Grid 12 (2) (2021) 1405–1415. doi:10.1109/TSG.2020.3026971.

[28] Z. Liang, Q. Alsafasfeh, T. Jin, H. Pourbabak, W. Su, Risk-Constrained Optimal Energy Management for Virtual Power Plants Considering Correlated Demand Response, IEEE Transactions on Smart Grid 10 (2) (2019) 1577–1587. doi:10.1109/TSG.2017.2773039.

[29] P. Scott, S. Thiébaux, M. Van Den Briel, P. Van Hentenryck, Residential demand response under uncertainty, in: International Conference on Principles and Practice of Constraint Programming, Springer, 2013, pp. 645–660. doi:https://doi.org/10.1007/978-3-642-40627-0_48.

[30] Y. Zheng, B. M. Jenkins, K. Kornbluth, A. Kendall, C. Træholt, Optimization of a biomass-integrated renewable energy microgrid with demand side management under uncertainty, Applied Energy 230 (2018) 836–844. doi:10.1016/j.apenergy.2018.09.015.

[31] Z. Wu, S. Zhou, J. Li, X. P. Zhang, Real-Time Scheduling of Residential Appliances via Conditional Risk-at-Value, IEEE Transactions on Smart Grid 5 (3) (2014) 1282–1291. doi:10.1109/TSG.2014.2304961.

[32] D. Zhu, G. Hug, Decomposed Stochastic Model Predictive Control for Optimal Dispatch of Storage and Generation, IEEE Transactions on Smart Grid 5 (4) (2014) 2044–2053. doi:10.1109/TSG.2014.2321762.

[33] D. Gao, Y. Sun, Y. Lu, A robust demand response control of commercial buildings for smart grid under load prediction uncertainty, Energy 93 (2015) 275–283. doi:https://doi.org/10.1016/j.energy.2015.09.062.

[34] M. G. Vayá, G. Andersson, S. Boyd, Decentralized control of plug-in electric vehicles under driving uncertainty, in: IEEE PES Innovative Smart Grid Technologies, Europe, 2014, pp. 1–6. doi:10.1109/ISGTEurope.2014.7028989.

[35] M. Diekerhof, F. Peterssen, A. Monti, Hierarchical Distributed Robust Optimization for Demand Response Services, IEEE Transactions on Smart Grid 9 (6) (2018) 6018–6029. doi:10.1109/TSG.2017.2701821.

[36] P. Scarabaggio, S. Grammatico, R. Carli, M. Dotoli, Distributed Demand Side Management With Stochastic Wind Power Forecasting, IEEE Transactions on Control Systems Technology (2021) 1–16doi:10.1109/TCST.2021.3056751.

[37] P. Kou, D. Liang, L. Gao, Stochastic Energy Scheduling in Microgrids Considering the Uncertainties in Both Supply and Demand, IEEE Systems Journal 12 (3) (2018) 2589–2600. doi:10.1109/JSYST.2016.2614723.

[38] E. Thomas, R. Sharma, Y. Nazarathy, Towards demand side management control using household specific Markovian models, Automatica 101 (2019) 450 – 457. doi:https://doi.org/10.1016/j.automatica.2018.11.057.

[39] C. Chen, J. Wang, S. Kishore, A Distributed Direct Load Control Approach for Large-Scale Residential Demand Response, IEEE Transactions on Power Systems 29 (5) (2014) 2219–2228. doi:10.1109/TPWRS.2014.2307474.

[40] M. Liu, Y. Shi, Model Predictive Control for Thermostatically Controlled Appliances Providing Balancing Service, IEEE Transactions on Control Systems Technology 24 (6) (2016) 2082–2093. doi:10.1109/TCST.2016.2535400.

[41] M. J. Fell, D. Shipworth, G. M. Huebner, C. A. Elwell, Public acceptability of domestic demand-side response in Great Britain: The role of automation and direct load control, Energy Research and Social Science 9 (2015) 72–84. doi:10.1016/j.erss.2015.08.023.

[42] K. Stenner, E. R. Frederiks, E. V. Hobman, S. Cook, Willingness to participate in direct load control: The role of consumer distrust, Applied Energy 189 (2017) 76–88. doi:https://doi.org/10.1016/j.apenergy.2016.10.099.

[43] PJM, Markets & Operations, https://www.pjm.com/markets-and-operations.aspx, Accessed: 20-10-2020.

[44] Australian Reneweable Energy Agency (ARENA), Demand Response RERT Trial Year 1 Report, https://arena.gov.au/assets/2019/03/demand-response-rert-trial-year-1-report.pdf, Accessed: 23-12-2019.

[45] B. Parrish, R. Gross, P. Heptonstall, On demand: Can demand response live up to expectations in managing electricity systems?, Energy Research & Social Science 51 (2019) 107–118. doi:https://doi.org/10.1016/j.erss.2018.11.018.

[46] The University of Queensland, Centre for Energy Data Innovation (CEDI), https://cedi.uqcloud.net.

[47] Energex, Air-conditioning rewards, https://www.energex.com.au/home/control-your-energy/positive-payback-program/positive-payback-for-business/air-conditioning-rewards, Accessed: 10-01-2020.

[48] M. Song, C. Gao, H. Yan, J. Yang, Thermal Battery Modeling of Inverter Air Conditioning for Demand Response, IEEE Transactions on Smart Grid 9 (6) (2018) 5522–5534. doi:10.1109/TSG.2017.2689820.

[49] Standards Australia, AS/NZS 4755.3.2-2012: Demand response capabilities and supporting technologies for electrical products, https://www.standards.org.au/standards-catalogue/sa-snz/electrotechnology/el-054/as-slash-nzs--4755-dot-3-dot-2-2012, Accessed: 02-01-2020.

[50] Ergon Energy, Eligible PeakSmart air conditioners, https://www.ergon.com.au/network/manage-your-energy/reward-programs/peaksmart-air-conditioning/eligible-peaksmart-air-conditioner-test, Accessed: 10-05-2021.

[51] A. Sheikhi, M. Rayati, S. Bahrami, A. M. Ranjbar, S. Sattari, A cloud computing framework on demand side management game in smart energy hubs, International Journal of Electrical Power & Energy Systems 64 (2015) 1007–1016. doi:https://doi.org/10.1016/j.ijepes.2014.08.020.

[52] A. Sheikhi, M. Rayati, S. Bahrami, A. Mohammad Ranjbar, Integrated Demand Side Management Game in Smart Energy Hubs, IEEE Transactions on Smart Grid 6 (2) (2015) 675–683. doi:10.1109/TSG.2014.2377020.

[53] A. Sheikhi, S. Bahrami, A. M. Ranjbar, An autonomous demand response program for electricity and natural gas networks in smart energy hubs, En-

ergy 89 (2015) 490–499. doi:https://doi.org/10.1016/j.energy.2015.05.109.

[54] N. Mahdavi, J. H. Braslavsky, Modelling and Control of Ensembles of Variable-Speed Air Conditioning Loads for Demand Response, IEEE Transactions on Smart Grid 11 (5) (2020) 4249–4260. doi:10.1109/TSG.2020.2991835.

[55] S. Shao, M. Pipattanasomporn, S. Rahman, Development of physical-based demand response-enabled residential load models, IEEE Transactions on Power Systems 28 (2) (2013) 607–614. doi:10.1109/TPWRS.2012.2208232.

[56] U.S. Energy Information Administration (EIA), Residential Energy Consumption Survey (RECS), https://www.eia.gov/consumption/residential/data/2015/, Accessed: 05-01-2020.

[57] U.S. Department of Energy, Storage Water Heaters, https://www.energy.gov/energysaver/water-heating/storage-water-heaters, Accessed: 05-01-2020.

[58] O. Brastein, D. Perera, C. Pfeifer, N.-O. Skeie, Parameter estimation for grey-box models of building thermal behaviour, Energy and Buildings 169 (2018) 58 – 68. doi:https://doi.org/10.1016/j.enbuild.2018.03.057.

[59] A. Afram, F. Janabi-Sharifi, Gray-box modeling and validation of residential HVAC system for control system design, Applied Energy 137 (2015) 134–150. doi:https://doi.org/10.1016/j.apenergy.2014.10.026.

[60] E. Calikus, S. Nowaczyk, A. Sant'Anna, H. Gadd, S. Werner, A data-driven approach for discovering heat load patterns in district heating, Applied Energy 252 (2019) 113409. doi:https://doi.org/10.1016/j.apenergy.2019.113409.

[61] A. Barbato, A. Capone, Optimization Models and Methods for Demand-Side Management of Residential Users: A Survey, Energies 7 (9) (2014) 5787–5824. doi:10.3390/en7095787.

[62] P. Scarabaggio, S. Grammatico, R. Carli, M. Dotoli, Distributed Demand Side Management With Stochastic Wind Power Forecasting, IEEE Transactions on Control Systems Technology (2021) 1–16doi:10.1109/TCST.2021.3056751.

[63] ENERNOC, The Demand Response Baseline, https://library.cee1.org/sites/default/files/library/10774/CEE_EvalDRBaseline_2011.pdf, Accessed: 02-02-2020.

[64] L. L. C. Gurobi Optimization, Gurobi Optimizer Reference Manual, http://www.gurobi.com (2021).

[65] Australian Energy Market Operator (AEMO), National Electricity Market (NEM) DATA DASHBOARD, https://aemo.com.au/en/energy-systems/electricity/national-electricity-market-nem/data-nem/data-dashboard-nem, Accessed: 24-03-2020.

[66] School of Earth and Environmental Sciences, The University of Queensland, UQ weatherstations, http://ww2.sees.uq.edu.au/uqweather/, Accessed: 20-04-2020.

[67] J. Löfberg, YALMIP : A Toolbox for Modeling and Optimization in MATLAB, in: In Proceedings of the CACSD Conference, Taipei, Taiwan, 2004.

[68] Ausgrid, Ausgrid Demand Management CoolSaver Interim Report, https://www.ausgrid.com.au/-/media/Documents/Demand-Mgmt/DMIA-research/Ausgrid-CoolSaver-Interim-Report-2017_Final.pdf, Accessed: 05-03-2020.

[69] Energex, PeakSmart events, https://www.energex.com.au/home/control-your-energy/managing-electricity-demand/peak-demand/peaksmart-events, Accessed 23-11-2019.